Contents lists available at ScienceDirect

Heliyon

Heliyon

Influence of nano-silica additions on hydration characteristics and cytotoxicity of calcium aluminate as biomaterial

H.K. Abd El-Hamid [*], M.M. Radwan

Refractories, Ceramics and Building Materials Department, National Research Centre (NRC), El-Buhouth St., Dokki, Cairo, 12622, Egypt

ABSTRACT

Composites of nano-calcium aluminate 'CA' biocement, synthesized by a solid state reaction, were prepared with 5, 10 and 20 wt.% of nano-SiO$_2$ particles. The influence of nano-SiO$_2$ particle additions on the physico-mechanical properties and hydration characteristics of CA biocement was studied. Calcium ion concentrations and, pH values of the curing medium were measured. The hydration characteristics of pure and composite CA phase were studied by determining the X-ray diffraction (XRD) and scanning electron microscopy (SEM) coupled with energy dispersive spectroscopy (EDS). Evaluation of cytotoxicity against the skin normal human cell line BJ-1 was carried out. The results showed that the bulk density and micro-hardness of the composite CA containing 10 wt.% of nano-SiO$_2$ were better than those of pure CA and composite prepared with higher weight percentages of nano-SiO$_2$. Both pure and composite CA bio-cements showed no cytotoxicity, making these materials suitable for medical applications.

1. Introduction

Cements used in orthopedics must satisfy many requirements, such as a low curing temperature, suitable setting time and high crushing strength. The most common materials that have been investigated for orthopedic and dentistry applications are called chemically–bonded ceramics (CBC), whose setting behavior is conducted by certain chemical reactions that can occur at room temperature [1]. Calcium aluminate cement (CAC) is classified as a CBC materials that has been used as a biomaterial with respect to its general physico-mechanical and biocompatible properties. Due to the high CaO content of CAC, it was stated that this material is very similar to bones and teeth [2, 3] and can be used in orthopedics for repairing bone and as dental restorative materials [4]. CAC overcomes some drawbacks of the commercial product mineral trioxide aggregate (MTA), which is used for root-end filling material purposes, such as long setting time, high porosity level, and low mechanical strength [5, 6].

Mono-calcium aluminate, CaO·Al$_2$O$_3$, is the main component of CAC. This ceramic material has special properties such as high early strength and resistance to elevated temperatures [7]. The superior mechanical properties of CAC at early hydration ages (24 h) make it a good material for load bearing in both medical and dental applications. The hydration products of calcium aluminate significantly depend on the curing

temperatures [8, 9]. The main hydrate, CAH$_{10}$, is formed at temperatures below 20 °C, whereas the main hydration products AH$_3$ and C$_2$AH$_8$ are found at 20 °C and above [10, 11, 12]. As CAH$_{10}$ and C$_2$AH$_8$ compounds are thermodynamically metastable, they have a higher solubility than the stable phases of C$_3$AH$_6$ and AH$_3$. When the stable phases start to nucleate, the metastable phases dissolve and further convert to the more stable C$_3$AH$_6$ and AH$_3$ phases with curing time and temperatures above 35 °C; this reaction is called the conversion reaction [13, 14]. Hydration reactions of CAC can be expressed by the following equations [12].

$$CA + 10H \rightarrow CAH_{10} \tag{1}$$

$$2CA + 11H \rightarrow C_2AH_8 + AH_3 \tag{2}$$

$$3CA + 12H \rightarrow C_3AH_6 + 2AH_3 \tag{3}$$

$$2CAH_{10} \rightarrow C_2AH_8 + AH_3 + 9H \tag{4}$$

$$3C_2AH_8 \rightarrow 2C_3AH_6 + AH_3 + 9H \tag{5}$$

At hot and humid conditions the conversion reactions increase leading to an increase in porosity, formation of micro-cracks and strength loss [7, 13]. Some studies have reported that the conversion reaction could be inhibited by micro-silica, fly ash [7], granulated blast-furnace slag [15], and sodium silicate [16] due to the formation of strätlingite compound C$_2$ASH$_8$. It was stated that strätlingite compound has higher mechanical

---

properties compared with hydrogarnet (C_3AH_6), which is formed during the conversion reaction [12, 17]. Bentsen *et al.* suggested that silica increases the formation of strätlingite and that the strätlingite compound crystallizes as a stable phase in the temperature range of 20–70 °C [18]. Similarly, Shiri *et al.* showed that nano-silica in mono-calcium aluminate improved its workability and strength [19].

The present work aims to study the influence of nano-silica particle additions on some characteristics of calcium aluminate cured at 37 °C to be used as a novel biomaterial in both dental and medical applications. Investigation of physico-mechanical properties, hydration characteristics and morphology of the hardened pastes were carried out. Additionally, the cytotoxicity of both pure and composite CA cement against the skin of normal human cell line BJ-1 was also determined.

2. Materials and methods

2.1. Materials preparation and characterization

A dry mixture of 1:1 $CaCO_3$ and Al_2O_3 ($CaCO_3$ (≈99.8%) and Al_2O_3 (≈99.6%) with higher purity) was used to formulate the CA phase. All chemicals were supplied by BDH Chemicals Ltd, Poole, England. The mixture was homogenized using an electric roller for 24 h and then pressed into 2 inch cubes and calcined at 1000 °C for 2 h in Vecstar electric furnace. The produced material was milled and then remolded into 2 inch cubes and fired at 1500 °C for 6 h [20, 21]. This solid state reaction was carried out in accordance to the phase diagram of calcium aluminate phases at a temperature needed for mono-calcium aluminate phase formation (CA) [12]. The resulting material was very finely ground for 15 h in an electric milling machine (Retsch GmbH PM100, Germany). This finely ground powder was characterized by its X-ray diffraction (XRD) pattern (Fig. 1). Transmission Electron Microscopy (TEM) ((JEM-1230) at 100 kV) was used to estimate the particle size (Fig. 2a).

Moreover, highly pure laboratory chemical nano-SiO_2 particles (≈99.8%) with grain size less than 20 nm (Fig. 2b) were used. Nano-SiO_2 particles were added to the CA powder in 0, 5, 10 and 20 wt.% and their abbreviations for identification are given as CA, CA/5S, CA/10S and CA/20S respectively. Distilled water (DW) was used as a mixing liquid to prepare the cement pastes. For suitable workable consistency, a water/powder ratio of 0.24 ml/g was employed. The cement pastes were prepared with the aid of cylindrical brass mold of dimensions: diameter = 10 mm and height = 2 mm. The paste was filled in the mold into two approximately equal layers. Each layer was compacted and pressed until a homogenous specimen was obtained. The samples were cured in 100% humidity chamber at a cons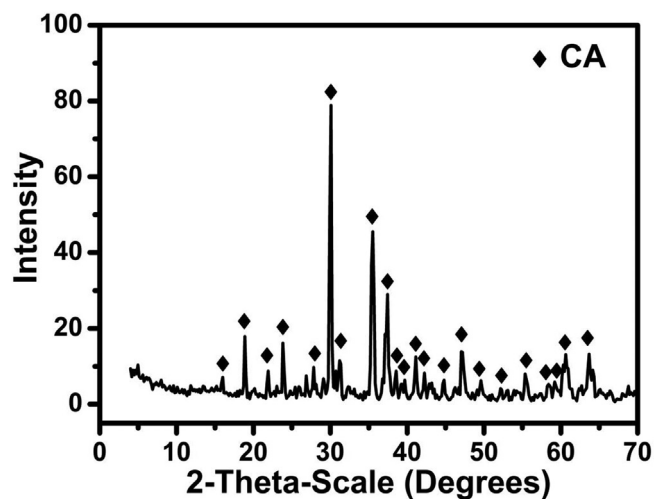tant temperature of 37 °C for 24 h directly after molding. The samples were de-molded and cured under DW at 37 °C until testing at 1, 3, 7 and 14 days.

2.2. Setting time

The final setting time of the synthesized CA biocement was performed using Vicat apparatus. One scoop (1 scoop = 0.2 g) of the freshly cement powder was mixed with one drop of DW (1 drop = 0.0482 g) and was placed into a mold that measured; 10 mm in height and 2 mm in thickness. Mixing was carried out on a glass slab with a stainless steel spatula, for 30 seconds. After 120 seconds from the start of mixing, a Gilmore needle (with a flat end diameter of 2 mm and weighting 100 g load) was gently lowered to the horizontal surface of the tested material. This procedure was repeated at 30-second intervals until the indenter failed to make a complete circular mark on the tested material. Three replicate specimens of the tested materials were made.

2.3. X-ray diffraction

Some selected samples were examined by XRD to identify the hydrated compounds with the aid of Bruker D8 Advance-Germany with X-Ray tube having a Cu Kα Target and radiation wavelength = 0.154nm, the X-ray was generated at 40 kV with a current of 2–5-mA. The XRD patterns obtained were converted to a series of lattice spacing d, Å and relative intensities (I/I^o) which were correlated with the relevant literature of JCPDS cards [22].

2.4. SEM-EDS analysis

Scanning electron microscopy (SEM) coupled with energy dispersive X-ray spectra (EDS) was carried out to examine the morphology of some selected hydrated samples by coating a thin layer of gold using an instrument (type Inspect S, T810, D8571, FEI Co., Japan) with an accelerating voltage of 30 kV and a magnification from 10× to 300000×.

2.5. Bulk density

The bulk density of the samples was measured at room temperature according to the Archimedes' method. The bulk density was determined by weighing the paste samples suspended in water and in air (saturated dry sample). Three replicate specimens of the tested materials were made. After the samples were dried at 100 °C for 24 h, the dried samples were weighed in air [23].

2.6. Micro-hardness test

The micro-hardness test was done by a Vickers indentation hardness tester with 1 kg load used for 15 seconds. The depth of indentation produced by a load on an indenter was measured [24]. The micro-hardness test was carried out on three cubes of each case of the hardened cement pastes.

2.7. pH of the immersion solution and calcium ion concentration

A half inch cube of each mix of cement paste was directly placed into 20 ml of DW to cover the paste [25]. Samples were kept at 37 °C in a 100% humidity water bath for 3, 7 and 14 days curing periods. The pH values of the immersion solution were determined using a solid-state pH sensor connected to a pH metre (Medika Scientific Jenway bench top pH meter, England). The concentration of Ca^{2+} ions in the curing medium was determined by atomic absorption spectrophotometer (Savant AA, GBC, Australia). An average of three samples were recorded.
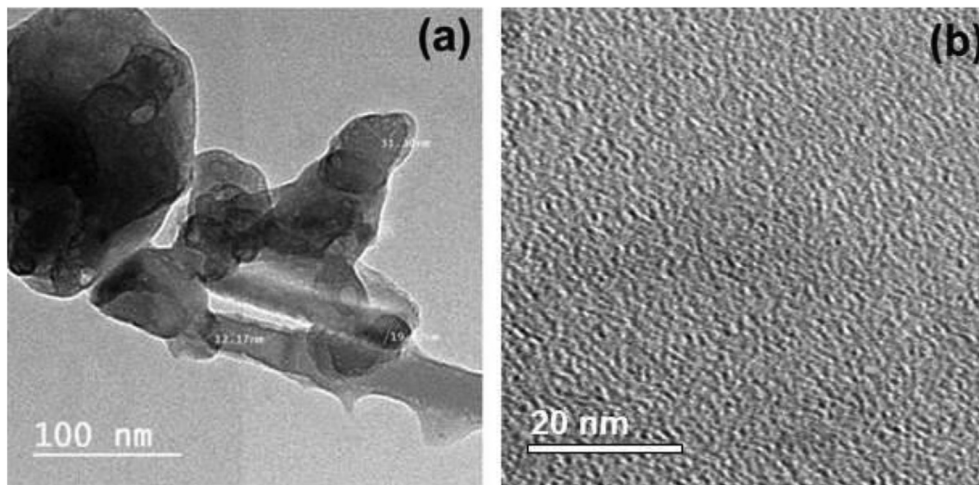

Fig. 1. XRD pattern of calcium aluminate (CA) powder fired at 1500 °C/6h.

Fig. 2. Transmission electron photomicrograph of the two experimental materials. (a) Calcium aluminate (CA) ranging from 12–31 nm and (b) nano-SiO_2 with a particle size below 20 nm.

2.8. Cytotoxicity test

2.8.1. Cell culture

The skin normal human cell line BJ-1 (a telomerase immortalized normal foreskin fibroblast cell line) was kept in Dulbecco's modified Eagle's medium (DMEM). The medium was supplemented with 10% fetal bovine serum and incubated at 37 °C in 5% CO_2 and 95% humidity. Cell was sub-cultured using trypsin 0.15%. The cell line was obtained from Karolinska Center, Department of Oncology and Pathology, Karolinska Institute and Hospital, Stockholm, Sweden.

2.8.2. Cell viability assay

After 24 h of seeding 50,000 cells per well in 96 well plates, the medium was replaced by complete medium containing a final concentration of the samples of 100 μg/ml in triplicate. The cells were cured for 48 h. Doxorubicin (100 μg/ml) was used as a positive control, and 0.5% dimethyl sulfoxide (DMSO) was used as a negative control. The cell viability was measured using the MTT (3-(4,5-dimethylthiazol-2-yl)-2,5-diphenyltetrazolium bromide) assay [26].
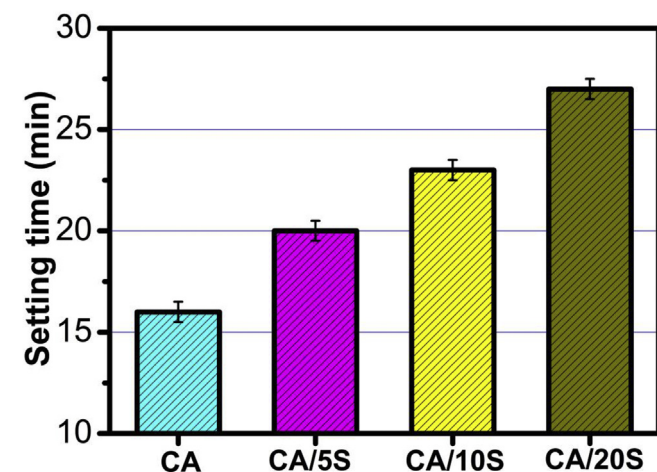
3. Results and discussion

3.1. Setting time

Fig. 3 represents the setting time values of pure and composites CA cement. The data showed a delayed setting time with an increase in the nano-silica content from zero to 20 wt.% as a result of the dilution effect of the CA phase by less chemically reactive material (SiO_2) [12]. The setting time values given in Fig. 3 were between 16 and 27 min, which is considered a good setting time for both dental and medical applications, as it is an appropriate range to handle such material. The setting and hardening processes of CAC start immediately after mixing with water during the first 24 h through first dissolution, followed by the precipitation of the major hydration phases CAH_{10}, C_2AH_8 and AH_3 [14, 27]

3.2. X-ray diffraction

The XRD patterns for the pastes of pure and composites CA cement (10, 20% of nano-SiO_2) cured at 37 °C for 14 days are represented in Fig. 4. The XRD patterns indicate the appearance of the characteristic
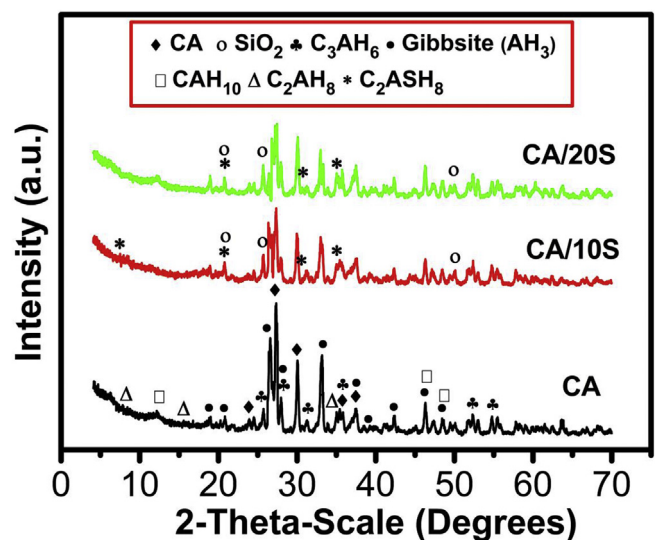

Fig. 3. The setting time values of CA cement containing 0, 5, 10 and 20 wt.% of nano-SiO_2 particles.

Fig. 4. XRD patterns of CA cement containing 0, 10, 20 wt.% of nano-SiO_2 particles cured for 14 days.
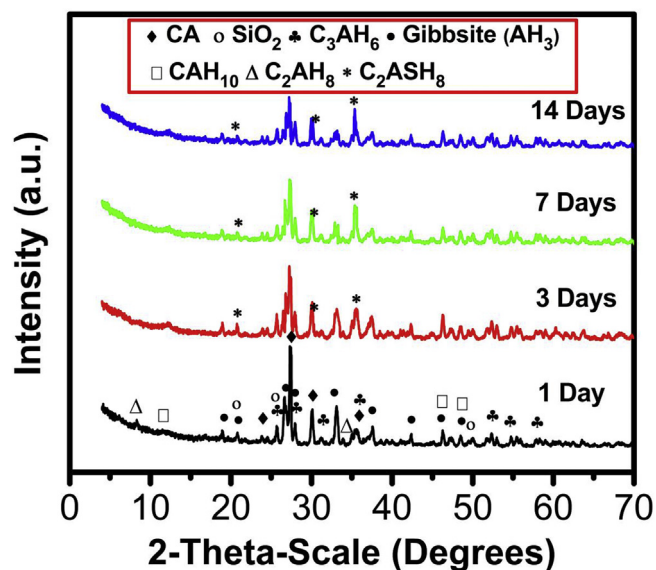
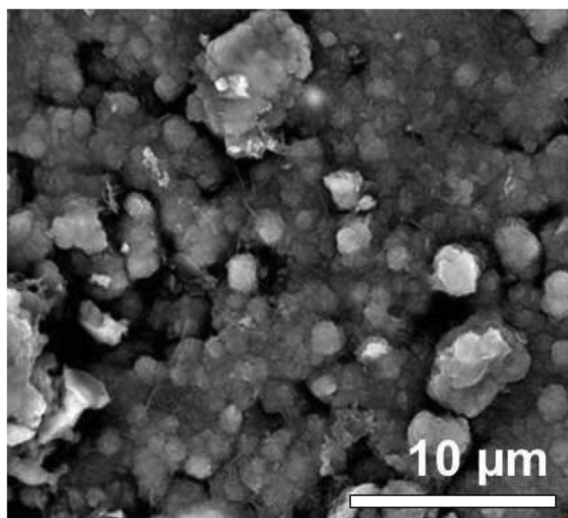**Fig. 5.** XRD patterns for CA cement containing 10 wt.% of nano-SiO$_2$ particles cured for 1, 3, 7 and 14 days.
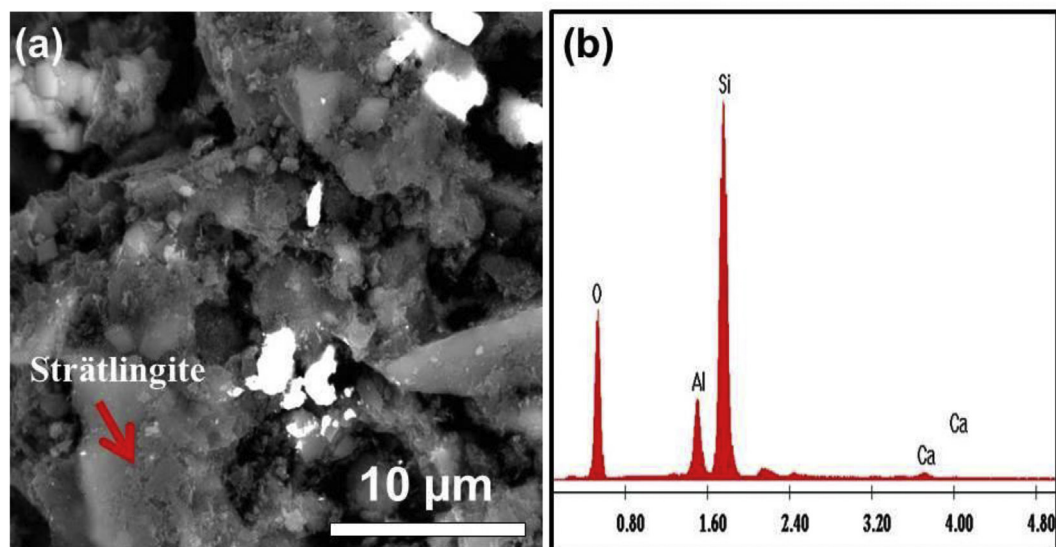

**Fig. 6.** SEM micrograph of pure CA cement cured for 14 days.

peaks of CAH$_{10}$ and C$_2$AH$_8$ phases together with those of the C$_3$AH$_6$ and AH$_3$ phases [12]. In pure CA cement, the characteristic XRD peaks of the CaO·Al$_2$O$_3$ anhydrous phase could be detected together with the C$_3$AH$_6$ and AH$_3$ phases. With the Addition of nano-SiO$_2$ particles, the characteristic peak intensities of hydrogarnet (C$_3$AH$_6$) and gibbsite (AH$_3$) decreased because the main hydrated phases of CA cement (CAH$_{10}$ & C$_2$AH$_8$) may react with the reactive nano-silica particles to form strätlingite (C$_2$ASH$_8$) according to the following equations [16, 28]:

$$2CAH_{10} + S \rightarrow C_2ASH_8 + AH_3 + 9H \quad (6)$$

$$C_2AH_8 + S \rightarrow C_2ASH_8 \quad (7)$$
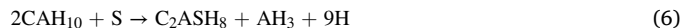
Therefore, the characteristic peaks of C$_2$ASH$_8$ slightly increased with diminishing hydrogarnet (C$_3$AH$_6$) and gibbsite (AH$_3$) peaks. The rate of C$_2$ASH$_8$ formation was controlled by the rate of silicate ion dissolution. When the amount of nano-silica increases to more than 10% in the CA cement, the intensities of the characteristic peaks of C$_2$ASH$_8$ are slightly diminished. This could be explained by the fact that when the percentages of nano-SiO$_2$ increase, the agglomeration of nanoparticles occurs and disrupts the hydration process [19].

Fig. 5 shows the XRD patterns of the hardened pastes of CA cement containing 10% nano-SiO$_2$ cured at 37 °C for 1, 3, 7 and 14 days. The XRD patterns indicate that by increasing the curing time there is an increase in the characteristic peaks of C$_2$ASH$_8$ and a decrease in the C$_3$AH$_6$ and AH$_3$ peaks as well as a diminishing of the intensity of the characteristic peaks of the anhydrous CaO·Al$_2$O$_3$ 'CA' phase.

3.3. SEM-EDS analysis

The micro structure of the pure CA cement cured at 37 °C for 14 days is shown in Fig. 6. The micrograph of the pure CA paste (in Fig. 6) illustrates the presence of highly crystalline cubic and granular crystals of C$_3$AH$_6$ as well as AH$_3$ gel. However, the micrograph of the CA paste containing 10% nano-SiO$_2$ cured at 37 °C for 14 days, as depicted in Fig. 7a, shows the presence of the thin flaky-plate like morphology of strätlingite hydrate (C$_2$ASH$_8$), which is stacked as parallel layers, in a more dense microstructure. The plates of C$_2$ASH$_8$ are deposited within the pore system, which leads to relatively higher physico-mechanical properties of these CA pastes containing 10% nano-SiO$_2$ [7].

Fig. 7b shows the corresponding EDS spectra of CA cement containing 10% nano-SiO$_2$. The EDS spectra emphasized the presence of Si atoms with the main elements of the spot analysis of the large plate-like crystals, namely, Al, O and Ca indicating the presence of an additional new hydration compound resulting from a reaction between the hydrated phases
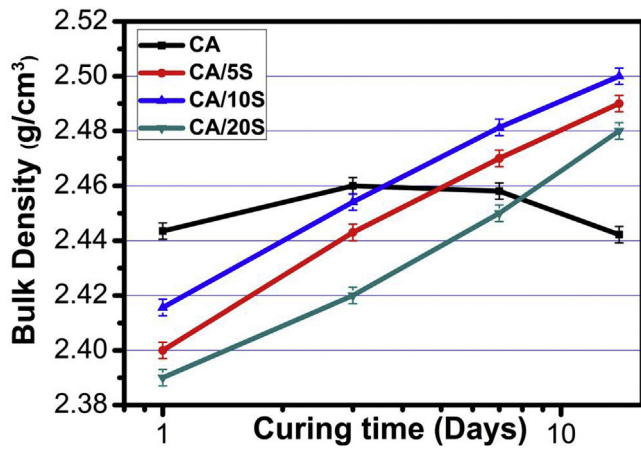

Fig. 7. (a) SEM micrograph and (b) EDS graph of CA cement containing 10 wt.% of nano-SiO$_2$ particles cured for 14 days.

Fig. 8. Bulk density of CA cement containing 0, 5, 10 and 20 wt.% of nano-SiO_2 particles against curing time.
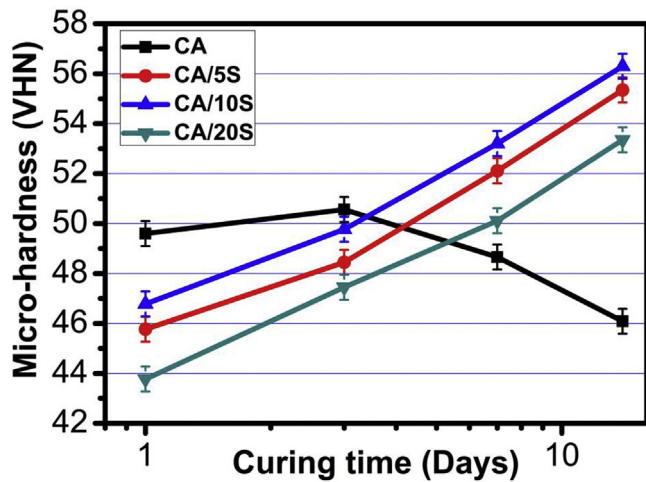

Fig. 9. Micro-hardness of CA cement containing 0, 5, 10, 20 wt.% of nano-SiO_2 particles against curing time.

(CAH$_{10}$ & C$_2$AH$_8$) of CA cement with active nano-silica particles to form a strätlingite compound (C$_2$ASH$_8$) [16]. These additional hydration phases were detected in the XRD analysis.

3.4. Bulk density

Fig. 8 illustrates the bulk density results of the hydrated sample pastes cured at 37 °C for 1, 3, 7 and 14 days. The density values of the pure CA cement increased with a curing age up to 3 days and then decreased at 7 and 14 days. However, for the CA cement composites, there was a steady increase in density values from 1 to 14 curing days. The cement composite containing 10% by weight nano-SiO_2 showed higher density values than 5 and 20% SiO_2 at all curing periods. The curing of CA cement under hot and humid conditions results in a process called the conversion process, in which the two main unstable hydrated phases CAH$_{10}$ and C$_2$AH$_8$ (hexagonal crystals), responsible for the mechanical and physical properties, will be converted to a more stable phase, namely, (cubic crystals) hydrogarnet (C$_3$AH$_6$) and gibbsite gel (AH$_3$), with low physico-mechanical properties, which will result in lower density values with curing age [29, 30].

Nano-silica particles may exhibit physical and chemical effects during the hydration process. One effect is the filling of the micro-pores, and the other is that the particles act as nucleating centers for the hydration reactants [19, 31]. Moreover, according to XRD results, the reactive nano-SiO_2 particles may react with CAH$_{10}$ and C$_2$AH$_8$ compounds to form
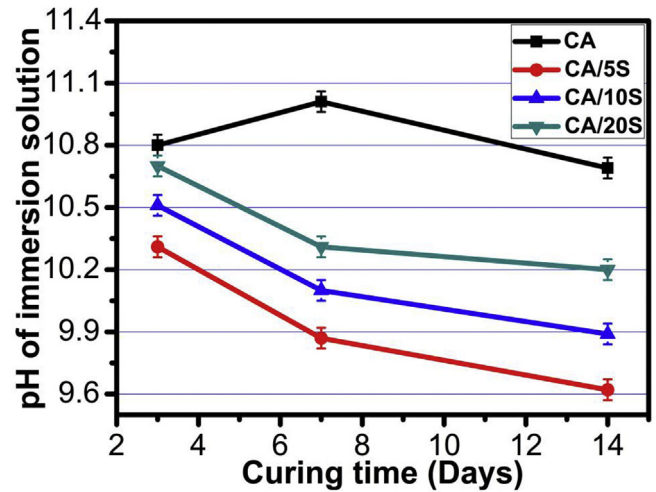

Fig. 10. pH changes after immersion of CA cement containing 0, 5, 10 and 20 wt.% of nano-SiO_2 particles against curing time.

the strätlingite compound (C$_2$ASH$_8$), which has good mechanical properties.

3.5. Micro-hardness test

Fig. 9 represents the micro-hardness results of the hydrated sample pastes cured at 37 °C for 1, 3, 7 and 14 days. The micro-hardness data indicate that the pure CA cement samples showed an increase in the micro-hardness values up to 3 days, followed by a decrease in micro-hardness at 7 and 14 days. However, the hardness values of the composites CA cement showed a continuous increase up to 14 days curing period. These results were confirmed by the bulk density data.

The results showed that the addition of 10% by weight nano-silica particles improved both the bulk density and micro-hardness because the microstructure of the hydrated cement pastes was more homogenous and dense than the pure CA, as observed in SEM results. However, with the further addition of nano-silica particles, the excess amounts of particles cannot be distributed well in the hardened cement paste, and weak zones may appear in the hydrated pastes. This effect is because nano-SiO_2 particles are very fine (<20 nm) and have a high surface area to volume ratio. Therefore, the homogenous hydration phases cannot be formed, and instead of improving the physico-mechanical properties of the samples, they negatively affect hydration, which is confirmed by the
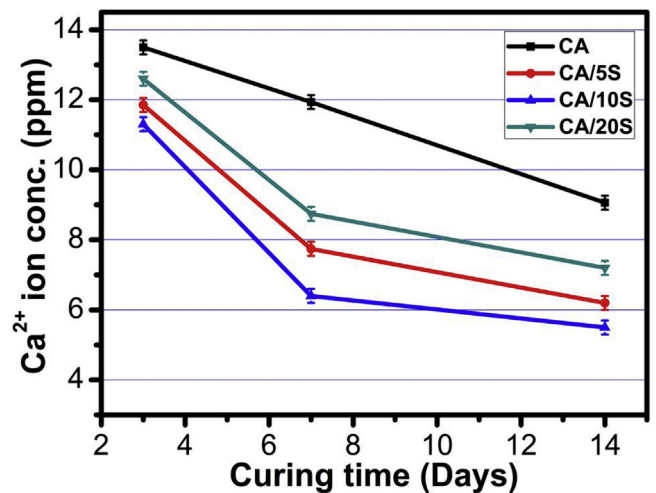

Fig. 11. Ca^{2+} ion concentration after immersion of CA cement containing 0, 5, 10 and 20 wt.% of nano-SiO_2 particles against curing time.
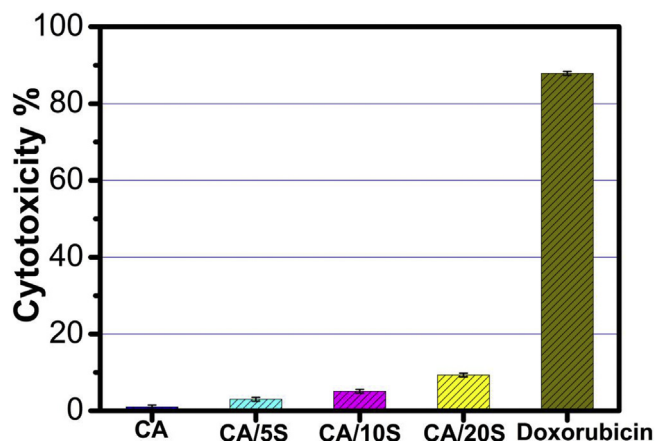
Fig. 12. Cytotoxicity of CA cement containing 0, 5, 10 and 20 wt.% of nano-SiO_2 particles after 48 h (at 100 μg/ml) on skin human normal cell line (BJ-1).

above XRD results given in Fig. 4 [7, 32].

3.6. pH of the immersion solution and calcium ion concentration

Fig. 10 represents the variations in pH of the immersion solution of pure and composites CA cement cured at 37 °C for 3, 7, 14 days. The pH values of the pure CA cement increase from 3 to 7 days, followed by a decrease from 7 to 14 days. This increase in the pH is mainly due to the conversion reactions of the CAH_{10} and C_2AH_8 compounds, which are thermodynamically metastable with a higher solubility to convert to the more stable C_3AH_6 and AH_3 compounds [13, 14]. The dissolution of the meta-stable hydrated phases (CAH_{10} and C_2AH_8) in the reaction medium may increase calcium and OH^- ions that are responsible for the increase in pH values [12]. However, in composites CA cement, there was a steady decrease in the pH values at all curing times. This decrease is due to the inhibition of the conversion reaction by the consumption of the dissolute calcium ions in the chemical reaction with the reactive SiO_2 particles [7].

The concentration of calcium ions in the immersion liquid for pure and composites CA cement cured at 37 °C for 3, 7 and 14 days is given in Fig. 11. The data show that the Ca^{2+} ions concentrations for the pure CA are higher than those of the composites CA. The concentration of Ca^{2+} ions slightly decreases in the case of pure CA at all curing times. However, in the case of composite CA cements, the concentration suddenly decreases from 3 to 7 days, followed by a slight decrease up to 14 days. The decrease in the calcium ion concentration was emphasized by the pH values. Generally, the CA phase has a low leakage since the material has a short setting time and good cohesiveness. The hydration process starts immediately via the dissolution of the CA phase in the aqueous curing medium producing Ca^{2+}, $Al(OH)_4^-$ and OH^- ions; this process is immediately followed by the precipitation of the less soluble hydrated phases [33, 34, 35].

3.7. Cytotoxicity test

Evaluation of the cytotoxicity of pure and composites CA cement against the skin normal human cell line (BJ-1) is given in Fig. 12. The culture of the cell line was treated for 48 h with samples at one concentration of 100 μg/ml. The data revealed that all investigated samples showed no cytotoxic effect against normal cells compared to the positive control (doxorubicin). The cytotoxicity test indicated that the pure and composites CA cement was completely safe for skin normal human cell line (BJ-1).

4. Conclusions

Calcium aluminate (CA) cement showed great potential in the biomaterial area due to its unique curing/hardening characteristics and related microstructure. The results showed that the addition of nano-SiO_2 particles to the CA cement plays an important role in inhibiting the conversion reactions of CA cement and consequently improving the physico-mechanical properties of the cement paste. The data showed that 10 wt.% of nano-silica was the optimum value to be mixed with CA cement that gave the best physico-mechanical results, good inhibition of the conversion reactions and a more dense microstructure. *The in vitro* cytotoxicity indicated that the pure and composites CA cement are safe on skin normal human cell line. Taking into consideration the results of this work, CA cement containing nano-silica is a potential candidate for biomedical applications.

Declarations

References

[1] R.M. Parreira, T.L. Andrade, A.P. Luz, V.C. Pandolfelli, I.R. Oliveira, Calcium aluminate cement-based compositions for biomaterial applications, Ceram. Int. 42 (10) (2016) 11732–11738.

[2] J. Lööf, Calcium- Aluminate as Biomaterial. Synthesis, Design and Evaluation, Dissertation, Faculty of Science and Technology-Uppsala University, Sweden, 2008, p. 87.

[3] J. Lööf, F. Svahn, T. Jarmar, H. Engqvist, C.H. Pameijer, A comparative study of the bioactivity of three materials for dental applications, Dent. Mater. 24 (2008) 653–659.

[4] L. Kraft, Calcium Aluminate Based Cement as Dental Restorative Materials, Dissertation, Faculty of Science and Technology-Uppsala University, Sweden, 2002, p. 65.

[5] VC. Pandolfelli, I.R. Oliveira, H.L. Rossetto, M. Jacobovitz, Aluminous Cement-Based Composition for Application in Endodontic Sand Cementitious Product Obtained Thereof, Patent Registration WO/2009/067774, 2009.

[6] I.R. Oliveira, V.C. Pandolfelli, M. Jacobovitz, Chemical, physical and mechanical properties of a novel calcium aluminate endodontic cement, Int. Endod. J. 43 (2010) 1069–1076.

[7] N.Y. Mostafa, Z.I. Zaki, O.H. Abd Elkader, Chemical activation of calcium aluminate cement composites cured at elevated temperature, Cement Concr. Compos. 34 (2012) 1187–1193.

[8] X. Shang, G. Ye, Y. Zhang, H. Li, D. Hou, Effect of micro-sized alumina powder on the hydration products of calcium aluminate cement at 40°C, Ceram. Int. 42 (2016) 14391–14394.

[9] N. Ukrainczyk, T. Matusinovic, S. Kurajica, B. Zimmermann, J. Sipusic, Dehydration of a layered double hydroxide-C_2AH_8, Thermochim. Acta 464 (2007) 7–15.

[10] W.E. Lee, W. Vieira, S. Zhang, Castable refractory concretes, Int. Mater. Rev. 46 (2001) 145–167.

[11] S.M. Bushnell-Watson, J.H. Sharp, On the cause of the anomalous setting behavior with respect to temperature of calcium aluminate cements, Cement Concr. Res. 20 (1990) 677–686.

[12] H.F.W. Taylor, Cement Chemistry, Academic Press, London, 1990, pp. 319–323.

[13] A.P. Luz, V.C. Pandolfelli, CaCO$_3$ addition effect on the hydration and mechanical strength evolution of calcium aluminate cement for endodontic applications, Ceram. Int. 38 (2012) 1417–1425.

[14] S.M. Bushnell-Watson, J.H. Sharp, The effect of temperature upon the setting behavior of refractory calcium aluminate cements, Cement Concr. Res. 16 (1986) 875–884.

[15] B. Singh, A.J. Majumdar, The hydration of calcium dialuminate and its mixtures containing slag, Cement Concr. Res. 22 (1992) 1019–1026.

[16] J. Ding, Y. Fu, J. Beaudoin, Study of hydration mechanisms in the high alumina cement-sodium silicate system, Cement Concr. Res. 26 (1996) 799–804.

[17] H.G. Midgley, Quantitative determination of phases in high alumina cement clinkers by X-ray diffraction, Cement Concr. Res. 6 (2) (1979) 217–223.

[18] S. Bentsen, A. Seltveit, B. Sanderg, Effect of Microsilica on Conversion of High Alumina Cement Calcium Aluminate Cement, Chapman and Hall, London (UK), 1990, p. 294.

[19] S. Shiri, M.H. Abbasi, A. Monshi, F. Karimzadeh, A study on mechanical and physical properties of monocalcium aluminate cement reinforced with nano-SiO$_2$ particles, Composites Part B 56 (2014) 30–33.

[20] J.M. Rivas Mercury, A.H. De Aza, P. Pena, Synthesis of CaAl$_2$O$_4$ from powders: particle size effect, J. Eur. Ceram. Soc. 25 (14) (2005) 3269–3279.

[21] S. Iftekhar, J. Grins, G. Svensson, J. Lööf, T. Jarmar, G.A. Botton, C.M. Andrei, H. Engqvist, Phase formation of CaAl$_2$O$_4$ from CaCO$_3$-Al$_2$O$_3$ powder mixtures, J. Eur. Ceram. Soc. 28 (2008) 747–756.

[22] R.W.M.D. Eye, E. Wait, X-ray Powder Photography in Inorganic Chemistry, Butter worths, London, 1960.

[23] ASTM Designation, C373-88 Water Absorption, Bulk Density, Apparent Porosity and Apparent Specific Gravity of Fired white ware Products, 1999.

[24] A.A. Eid, T. Komabayashi, E. Watanabe, T. Shiraishi, I. Watanabe, Characterization of the mineral trioxide aggregate–resin modified glass ionomer cement interface in different setting conditions, J. Endod. J 38 (2012) 1126–1129.

[25] J. Nurit, J. Margerit, A. Terol, P. Boudeville, PH-metric study of the setting reaction of mono phosphate monohydrate/calcium oxide-based cements, J. Mater. Sci. Mater. Med. 13 (1993) 1007–1014.

[26] T. Mosmann, Rapid colorimetric assay for cellular growth and survival: application to proliferation and cytotoxicity assays, J. Immunol. Methods 65 (1) (1983) 55–63.

[27] W.N. Liu, J. Chang, Y.Q. Zhu, M. Zhang, Effect of tricalcium aluminate on the properties of tricalcium silicate-tricalcium aluminate mixtures: setting time, mechanical strength and biocompatibility, Int. Endod. J. 44 (1) (2010) 41–50.

[28] H.M. Son, S.M. Park, J.G. Jang, H.K. Lee, Effect of nano-silica on hydration and conversion of calcium aluminate cement, Constr. Build. Mater. 169 (2018) 819–825.

[29] T. Matrusinovic, J. Sipusic, N. Vrbos, Porosity-Strength relation in calcium aluminate cement pastes, Cement Concr. Res. 33 (11) (2003) 1801–1806.

[30] O. Seung-Han, C. Se-Young, L. Yong-Keun, N.K. Kyoung, Preparation of calcium aluminate cement for hard tissue repair: effects of Lithium fluoride and maleic acid on setting behavior, compressive strength, and biocompatibility, J. Biomed. Mater. Res. 62 (2002) 593–599.

[31] H. Li, H.G. Xiao, J.P. Ou, A study on mechanical and pressure-sensitive properties of cement mortar with nanophase materials, Cement Concr. Res. 34 (2004) 435–438.

[32] N.Y. Mostafa, Q. Mohsen, S.A.S. El-Hemaly, S.A. El-Korashy, P.W. Brown, High replacements of reactive pozzolan in blended cements: microstructure and mechanical properties, Cement Concr. Compos. 32 (2010) 386–391.

[33] W. Khaliq, H.A. Khan, High temperature material properties of calcium aluminate cement concrete, Constr. Build. Mater. 94 (2015) 475–487.

[34] M.M. Radwan, H.K. Abd EL-Hamid, H.H. Abo-almaged, H.N. Salem, N. Omar, Evaluation of calcium aluminate/calcium phosphate based bio-cements as root-end filling material, Orient. J. Chem. 33 (6) (2017) 2692–2706.

[35] I.R. Oliveira, T.L. Andrade, K.C.M.L. Araujo, A.P. Luz, V.C. Pandolfelli, Hydroxyapatite synthesis and the benefits of its blend with calcium aluminate cement, Ceram. Int. 42 (2016) 2542–2549.